



Green Synthesis of Cyclic Carbonates from Epoxides and CO₂ Using Transition Metal Substituted Polyoxometalate-PDDA Hybrid Catalysts

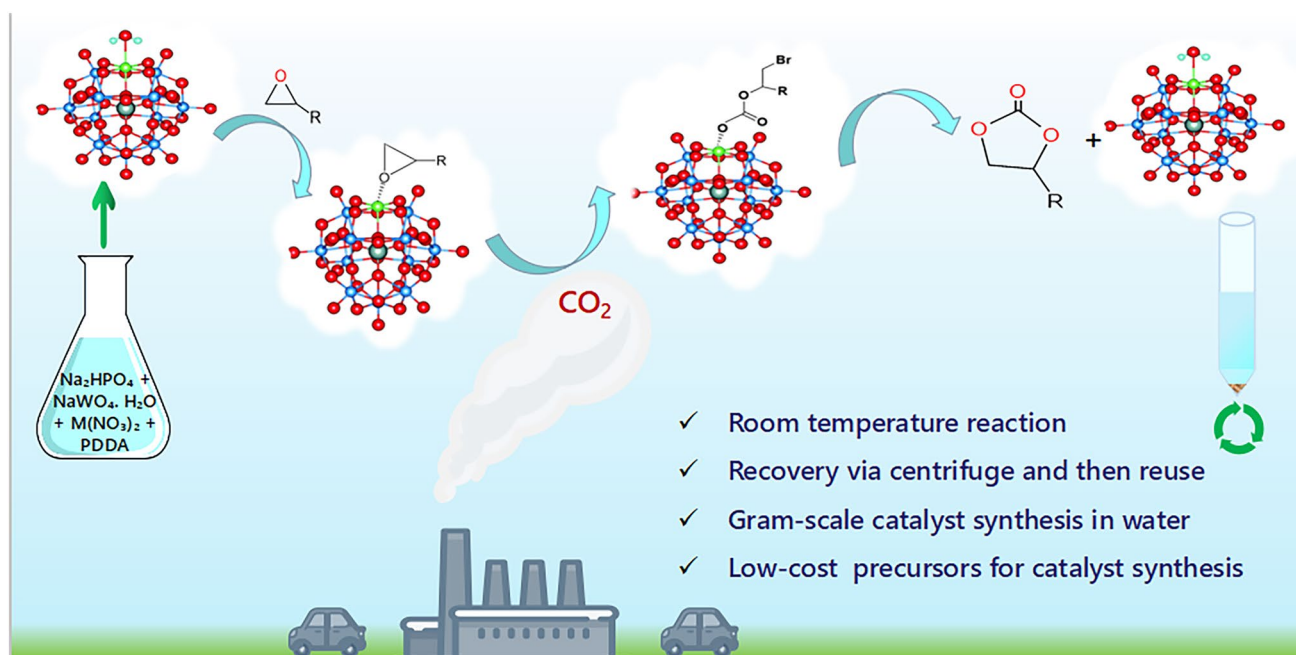
Rehana Jan¹ · Christy Ann Biji² · K. Shakeela¹ · Rafik Rajjak Shaikh¹ · G. Ranga Rao³

Received: 9 April 2023 / Accepted: 14 June 2023 / Published online: 19 July 2023
© The Author(s), under exclusive licence to Springer Science+Business Media, LLC, part of Springer Nature 2023

Abstract

Polyoxometalates can be tuned for specific catalytic property by substituting transition metal ions. We report the synthesis of hybrid materials of Cu²⁺, Co²⁺ and Ni²⁺ substituted phosphotungstates and poly(diallyldimethylammonium) chloride polymer (PDDA) for CO₂ fixation. The in situ generated transition metal substituted polyoxometalates (TMS-POMs) are analyzed by FTIR, powder XRD, ³¹P NMR and SEM techniques. The hybrid TMS-POM materials are found to be good catalysts for converting epoxides to cyclic carbonates. Among these, PDDA-PWCo is the most efficient catalyst for cycloaddition of CO₂ under solvent-free conditions at room temperature in shortest reaction time. Only 0.2 mol% of PDDA-PWCo is enough to deliver 100% conversion and selectivity to cyclic carbonates. This catalytic approach is employed for conversion of other cyclic, acyclic, and aromatic epoxides without using column purifications. Overall, the method of obtaining cyclic carbonates under green conditions using TMS-POMs-PDDA hybrid materials appears suitable for industrial applications.

Graphical Abstract



Keywords CO₂ conversion · Epoxides · Cyclic carbonates · Polymer · PDDA · Transition-metal substituted polyoxometalate

Extended author information available on the last page of the article

1 Introduction

The eco-friendly production of valuable chemicals is one of the best methods for CO₂ fixation. In this context, capture and conversion of CO₂ to valuable chemicals such as cyclic carbonates is considered as a feasible and efficient catalytic process [1–5]. Carbon dioxide is considered to be a thermodynamically stable molecule, and thus, higher energy supply and harsh reaction conditions are usually expected to drive CO₂ conversion such as high reaction temperature and pressure, extremely reactive substrates and reagents. Thus, it is necessary to develop catalysts with higher efficiency for cost effective conversion of CO₂ under mild reaction conditions. The synthesis of cyclic carbonates from epoxide and CO₂ stands as atom-economic, environmentally friendly and green approach for the conversion and storage of CO₂ [6–8]. In order to facilitate the synthesis of cyclic carbonates, various metal oxides, salen complexes, porous catalysts, organic and inorganic bases, titanosilicates, zeolites, and many metal/organic-supported complexes have been employed [8, 9]. Heterogeneous catalysts are preferred because of simple work-up procedures involved and their recyclability [10, 11]. Polyoxometalate-based hybrid materials are promising heterogeneous catalysts for CO₂ conversion to valuable products and intermediates such as polycarbonates, cyclic carbonates and carboxylic acids [12–14].

Polyoxometalates (POMs) are metal–oxygen anionic cluster materials with varied structural characteristics and versatile functionalities useful for catalysis and photochemical reactions [15–18]. The stable Keggin-type POMs contain twelve metal-oxoctahedra assembled around a tetrahedral oxo-anion with generic formula $[(X^{n+}M_{12}O_{40})]^{-(8-n)}$ where M = Mo, W and X = Si, P. These clusters assemble in acidic medium (pH < 3). Lacunary polyoxometalates (L-POMs) represent an important sub-class of POMs that are synthesized by removing one or more of the MO_x units from parent polyoxometalate cluster $[XM_{12}O_{40}]^{n-}$, thus producing mono- and polylacunary POMs, respectively [14, 19–26]. The L-POMs have enhanced properties than parent POMs because of the removal of MO_x octahedral moieties from the saturated Keggin anion structure. The increased anionic charge and nucleophilic oxygen enriched surface of L-POMs allow its interactions with various cations. Incorporation of transition metals into the defect sites of the L-POMs results in a whole new array of transition metal substituted polyoxometalates (TMS-POMs) with improved catalytic and other properties depending on the metal ions incorporated. The formation of these species are highly pH dependent, each possessing unique reactivity as well as stability trend [19].

However, POMs as catalysts have a few drawbacks that include difficulty in catalyst/product separation, product

contamination and poor processability which are crucial factors for environmental sustainability. One of the typical methods to overcome these shortcomings is to integrate the POMs into suitable polymer matrixes having counter cationic groups that can help to exploit the intrinsic anionic character of POMs [20]. Proper combination of POMs with polymer matrices can give rise to materials for wide variety of applications [27, 28]. Polyelectrolytes are a certain group of organic polymers that can deposit on solid surfaces and colloids through electrostatic interactions [29]. Poly(diallyldimethylammonium) chloride (PDDA) is one such organic polymer that can be used as a polymer matrix to immobilize the POMs. The electrostatic interactions between the organic substrate and catalytic center of POM can enhance the stability and catalytic efficiency of the resultant hybrid material [21, 22].

POM-based materials have been employed previously for catalytic conversion of CO₂ and epoxides to cyclic carbonates [14, 30]. The POM based compounds are good catalysts as these materials activate the epoxides/CO₂ by interacting with the basic oxygen atoms and acidic metal sites [14, 23, 24]. Structural and functional modification of polyoxometalate clusters can lead to POM-based hybrids that are promising eco-friendly heterogeneous catalysts for the cycloaddition reaction of CO₂ and epoxides. We have synthesized three PDDA-metal substituted monolacunary phosphotungstate (PDDA-TMSPOM) hybrid materials (PDDA-PWCo, PDDA-PWNi, and PDDA-PWCu) as catalysts for CO₂ conversion into cyclic carbonates under solvent-free ambient reaction conditions. These POM-hybrid materials are found to be active and PDDA-PWCo is the best catalyst among them for CO₂ conversion.

2 Experimental

2.1 Materials

Sodium tungstate (Na₂WO₄·2H₂O) salt is purchased from Avra Laboratories, India. Disodium hydrogen phosphate (Na₂HPO₄), nitrate salts of cobalt, nickel and copper and phosphotungstic acid (H₂PW₁₂O₄₀) were purchased from Thermo Fisher Scientific, India, and Poly(diallyldimethylammonium) chloride PDDA was supplied by Aldrich. These precursor salts are used in the preparation TMS-POMs hybrid materials.

2.2 Synthesis of PDDA-TMS-POM Hybrid Materials

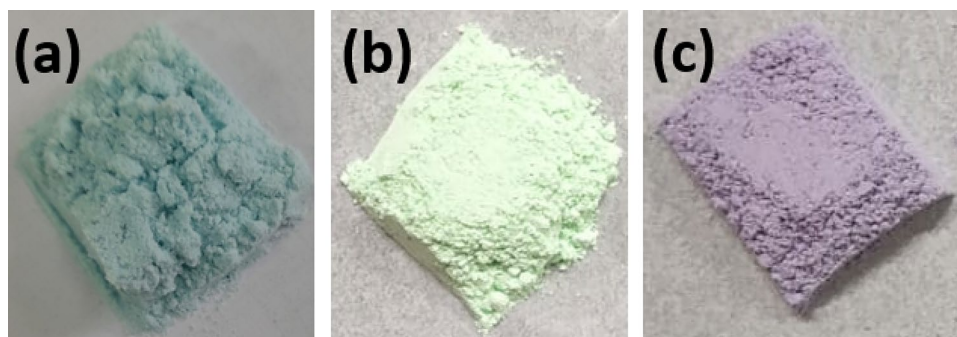
The in situ synthesis of Keggin-based TMS-POM hybrid catalysts were carried out following the literature report [31]. Typically, 2.0 mmol of disodium hydrogen phosphate, 25 mmol of sodium tungstate and 3 mmol of metal nitrate

(Co²⁺, Ni²⁺ and Cu²⁺) were dissolved in 50 ml distilled water. The pH of the solution was maintained at 4.8 using 1.0 M HNO₃. The resultant solution contains the transition metal substituted Keggin ions. In the next step, the above solution is mixed with 5 ml of poly(diallyldimethylammonium) chloride (PDDA). The reaction was carried out under stirring conditions for 1 h. The resulting precipitate was washed, filtered and dried. These TMSPOM-POM hybrid materials are denoted as PDDA-PWCo, PDDA-PW_{Ni} and PDDA-PWCu respectively. The three PDDA-TMSPOM hybrid materials are soft and powdery in nature. The substituted transition metal contributes the characteristic colour to the compounds. Accordingly, the colours of the compounds, PDDA-PWCu, PDDA-PW_{Ni} and PDDA-PWCo are light blue, light green and plum color, respectively (Fig. 1).

2.3 Materials Characterization

The FTIR spectra of the samples were collected from JASCO FT/IR 4100 spectrometer adopting KBr pellet method. The UV–Visible analyses of the samples were conducted on JASCO V-660 spectrometer using BaSO₄ as a reference in the range of 200–800 nm. Powder X-ray diffraction (PXRD) patterns of the hybrid materials were obtained using Bruker D8 Advance X-ray diffractometer employing Cu K α ($\lambda = 0.15406$ nm) radiation. The microscopic studies were carried out using FEI Quanta 200F electron microscope. The samples were subjected to differential thermal analysis (DTA) and thermogravimetric analysis (TGA) in Perkin-Elmer, TGA Q500 machine in nitrogen flow. The ³¹P NMR analyses of the hybrid catalyst materials were done in solid state mode using Bruker-FT-NMR 400 MHz spectrometer. The X-ray photoelectron spectroscopy (XPS) measurements were recorded using an ESCA probe TPD spectrometer from Omicron Nanotechnology, with an X-ray source of 1486.6 eV from polychromatic Al K α radiation. The catalytic conversions of CO₂ to cyclic carbonates were analyzed by ¹H NMR spectra recorded on Bruker-FT-NMR 500 MHz spectrometer. The reaction mixtures were dissolved in CDCl₃ solvent for NMR analysis.

Fig. 1 Powder samples of transition metal substituted POM-based hybrid catalytic materials, (a) PDDA-PWCu, (b) PDDA-PW_{Ni} and (c) PDDA-PWCo



3 Results and Discussion

3.1 Physicochemical Characterization

Figure 2 shows the FT-IR spectra of the three PDDA-TMSPOM hybrid materials. The IR spectrum of pure phosphotungstic acid is also included in order to compare the Keggin signature peaks. The peaks at 807, 892, 988 and 1080 cm⁻¹ correspond to the stretching frequencies of (W – O_e – W), (W – O_c – W), (W = O_{Ter}) and (P – O), respectively, signifying the formation of Keggin structure [25]. The intense peak at 1080 cm⁻¹ is due to the (P – O) vibration of the PO₄ unit in the center of parent Keggin anion. However, this peak bifurcated in the hybrids, due to the loss of symmetry of PO₄ tetrahedral unit, as a result of metal substitution. This splitting of P–O band clearly indicates the formation of lacunary PW₁₁. Thus, the FT-IR spectral signatures of Keggin ions indicate clearly that the transition metal ion is occupying the octahedral site inside the Keggin structure and not present as a counter ion [26]. The spectra show the characteristic absorption bands of asymmetrical and

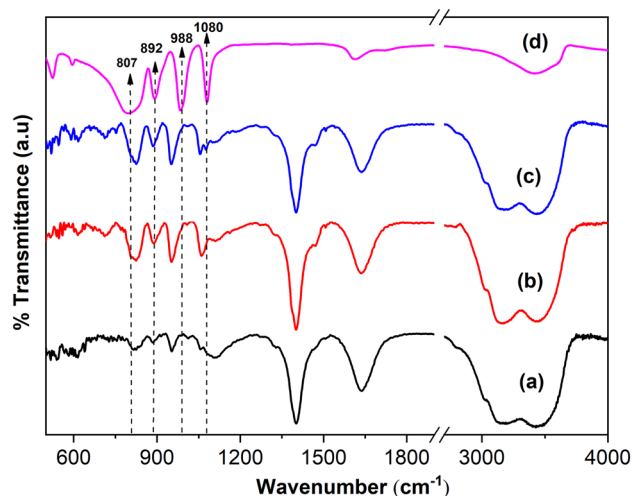


Fig. 2 FT-IR spectra of (a) PDDA-PWCu, (b) PDDA-PW_{Ni}, (c) PDDA-PWCo and (d) pure H₃PW₁₂O₄₀ (PWA)

symmetrical stretching frequencies of $-\text{CH}_2-$ at 3012 cm^{-1} and 2814 cm^{-1} , respectively, while the significant peak at 1400 cm^{-1} is attributed to $-\text{CH}_2-$ alkyl rocking vibrations present in PDDA moiety. The strong broad peaks at 3154 cm^{-1} and 3435 cm^{-1} are due to stretching of N–H and O–H, respectively [32].

The UV-Visible absorption spectra of hybrid materials are shown in Figure 3. Polyoxometalates show significant oxygen-to-metal charge transfer phenomenon in the UV region [26]. The three peaks at 210 nm, 260 nm and 310 nm correspond to the oxygen to tungsten charge transfer associated with the edge-sharing and corner-sharing oxygen of the Keggin units. The 3d metal substitution in the Keggin unit resulted in absorbance in the visible region. The green colour of PDDA-PW₁₁Ni and blue colour of PDDA-PW₁₁Cu containing Ni²⁺ and Cu²⁺ ions, respectively, show absorption in the region 650–800 nm and beyond. These broad bands are due to the d-d transitions of d⁸ (Ni²⁺) and d⁹ (Cu²⁺) ions. The plum colour of PDDA-PW₁₁Co indicates the substitution of Co²⁺ ions and show broad absorption band in the range of 470–650 nm.

The absorbance features obtained between 400 to 800 nm visible regions are attributed to the d–d transitions occurring in the 3d transition metal ions which are found to be occupying the octahedral site created in the monolacunary Keggin ion. Further, the diffuse reflectance features in the UV region are matching with the parent Keggin ion. This indicates that the electronic properties of parent Keggin structure remain unaltered in the UV region by the substitution of 3d metal ions in the octahedral moiety of monolacunary Keggin units.

The powder XRD patterns of these hybrid materials presented in Figure 4 reveal the amorphous nature of these materials. Phosphotungstic acid (PWA) is known for its

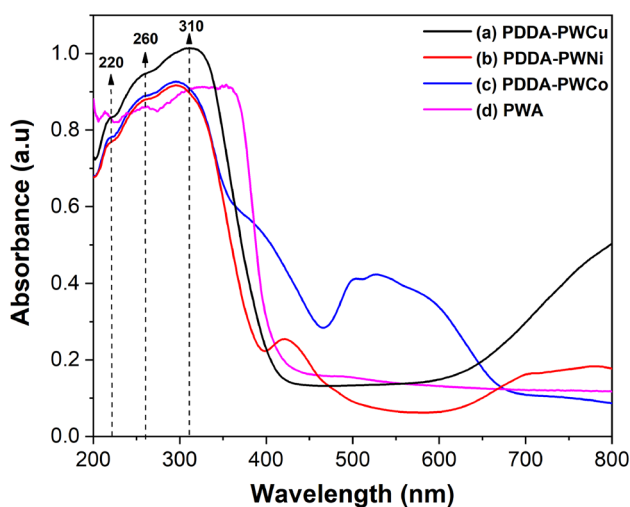


Fig. 3 UV-Visible spectra of (a) PDDA-PW₁₁Cu, (b) PDDA-PW₁₁Ni, (c) PDDA-PW₁₁Co and (d) H₃PW₁₂O₄₀ (PWA)

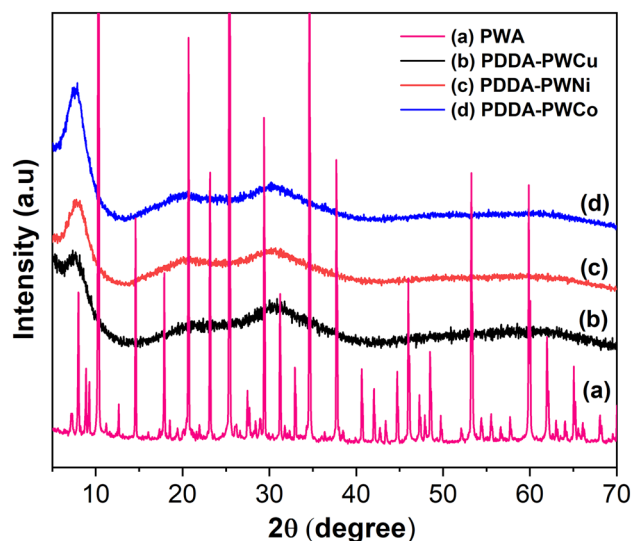


Fig. 4 Powder XRD pattern of (a) PWA, (b) PDDA-PW₁₁Cu, (c) PDDA-PW₁₁Ni and (d) PDDA-PW₁₁Co

crystalline nature (Figure 4a), while the resulting hybrid materials do not show intense peaks in the higher angle region [29]. The polymeric PDDA chains interact with metal substituted Keggin units, thereby the regular spacing between them increases and crystallinity decreases. The diffraction peaks have broadened and merged into the lower region, which specify the amorphous nature of the hybrid material [29]. These hybrid materials have intense peak at around $2\theta=7.5$. This indicates the presence of short range order with open and layered structure and d-spacing of the layered structure is calculated to be 1.17 nm. The particle sizes of PDDA-PW₁₁Cu and PDDA-PW₁₁Ni samples calculated using the Scherrer equation are of found to be about 3 nm in size.

All the hybrid materials show similar stepwise decomposition pattern as seen in Figure 5. PDDA is purely organic and it shows two step decomposition in the range of 350–550 °C. The weight loss in hybrid materials till 120 °C is due to the loss of adhered water molecules. The next two-step weight loss is observed between 300–450 °C and 600–750 °C, which is due to the loss of organic moiety, PDDA present in the hybrid materials [32]. The enhanced stability of the PDDA polymeric moiety can be attributed to the strong electrostatic interaction with Keggin anions. All the hybrid materials show 15 to 20% of weight loss, which can be correlated with the interaction of each metal substituted Keggin (PW₁₁O₃₉M)⁵⁻ with five monomeric units of PDDA. This in turn proves the formation of hybrid material of metal substituted Keggin and PDDA. Furthermore, metal substituted Keggin also shows extended thermal stability up to 750 °C, which later decomposes to its oxides.

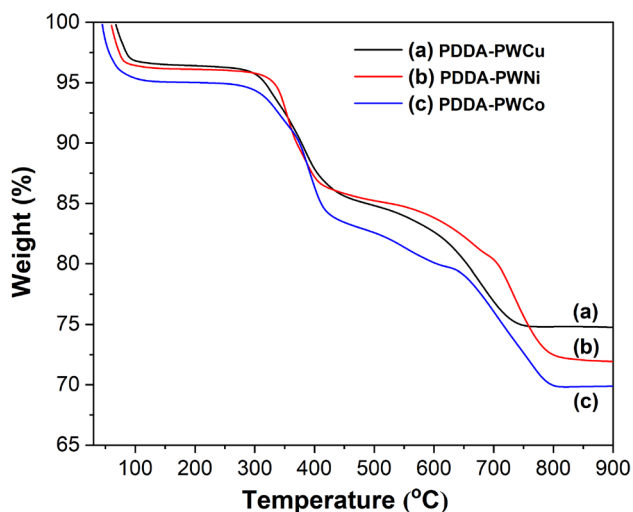


Fig. 5 Thermogravimetric analysis of (a) PDDA-PWCo, (b) PDDA-PWCo and (c) PDDA-PWCo

The surface morphologies of the hybrid materials are studied by scanning electron microscopy and the images along with their respective EDAX spectra are shown in Figure 6. As explained from powder XRD patterns, these hybrid materials show amorphous morphologies. The PDDA-TMSPOM hybrid materials seem to have aggregated particles. The modification of the pure PWA by metal substitution and PDDA functionalization has resulted in the

change in morphology. The PDDA-TMSPOM are composed of non-uniform particles in irregular layers. The insets in Figure 6 show closer magnification, where Figure 6a showing PDDA-PWCo has similar morphology, while Figure 6b showing PDDA-PWCo has wavy texture in its inset and Figure 6c showing PDDA-PWCo has layered morphology (inset image). Further, the EDAX data in Figure 6 shows the presence of respective substituted metal ions in the hybrids and the composition corroborates that the hybrid materials are formed by the interaction of five monomeric units of PDDA each metal substituted Keggin ($PW_{11}O_{39}M$)⁵⁻, which is also determined through TGA (Figure 5).

The 3d metal substituted Keggin ions are formed in situ during the synthesis of hybrid materials. In general, the unsubstituted Keggin, ($PW_{12}O_{40}$)³⁻, has a chemical shift of -15.1 ppm [33], whereas monolacunary Keggin is deshielded to -10 ppm [34]. The 3d metal present in the lacuna of Keggin structure shows a characteristic peak at -13.1 ppm [26, 35]. In Fig. 7, the ³¹P NMR of the three hybrid materials show -13.80 , -13.72 and -13.83 ppm for PDDA-PWCo, PDDA-PWCo and PDDA-PWCo, respectively. This unequivocally confirms the metal substitution in the Keggin structure.

The core level XPS of the PDDA-PWCo hybrid material has been recorded to analyse the elements present in the hybrid. The full survey spectrum shown in Fig. 8a is evident of the presence of W 4f, P 2p, C 1s, O 1s and Co 2p. The C 1s and O 1s are arising from the polymeric chains of PDDA

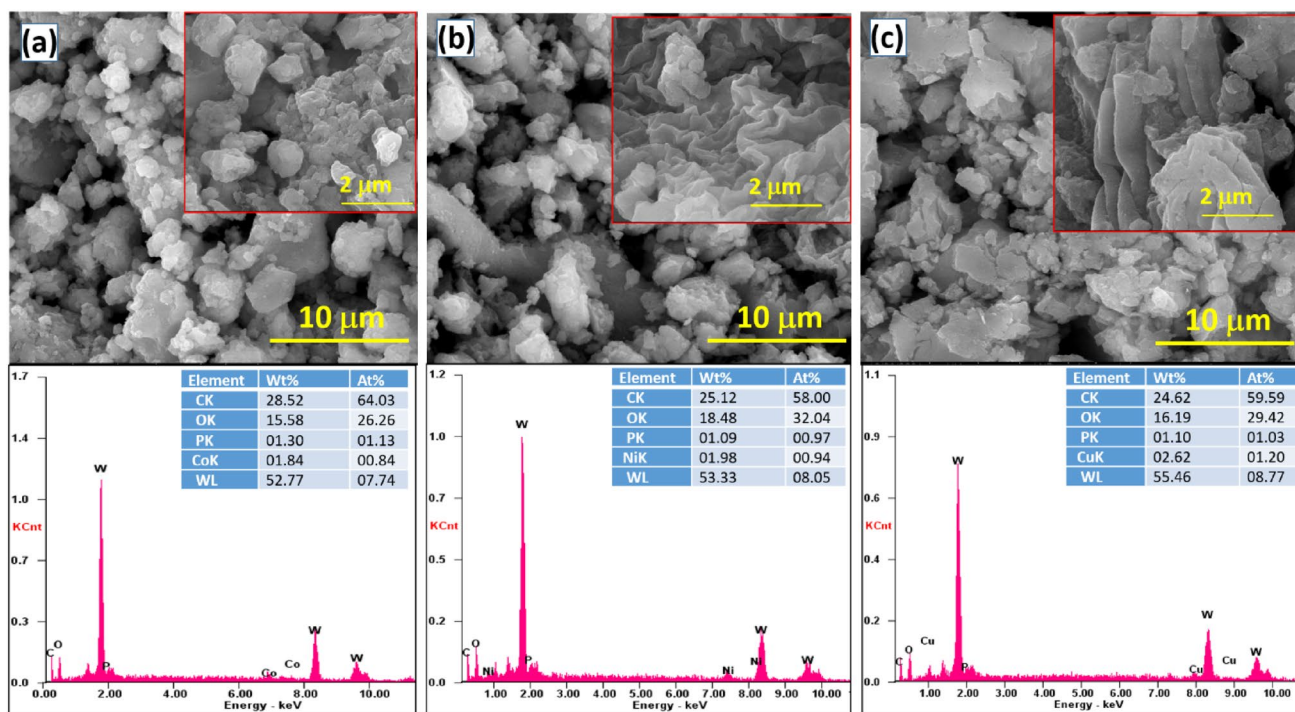


Fig. 6 SEM images and EDAX analysis of (a) PDDA-PWCo, (b) PDDA-PWCo and (c) PDDA-PWCo

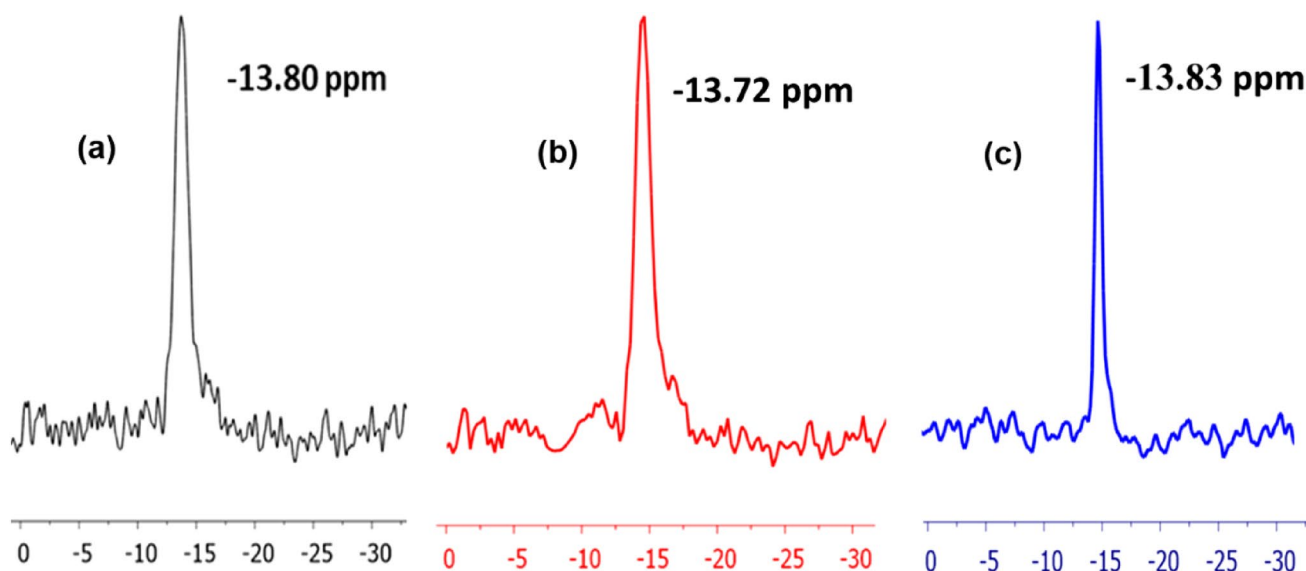


Fig. 7 ^{31}P NMR of (a) PDPA-PWCu, (b) PDPA-PWNI and (c) PDPA-PWCo

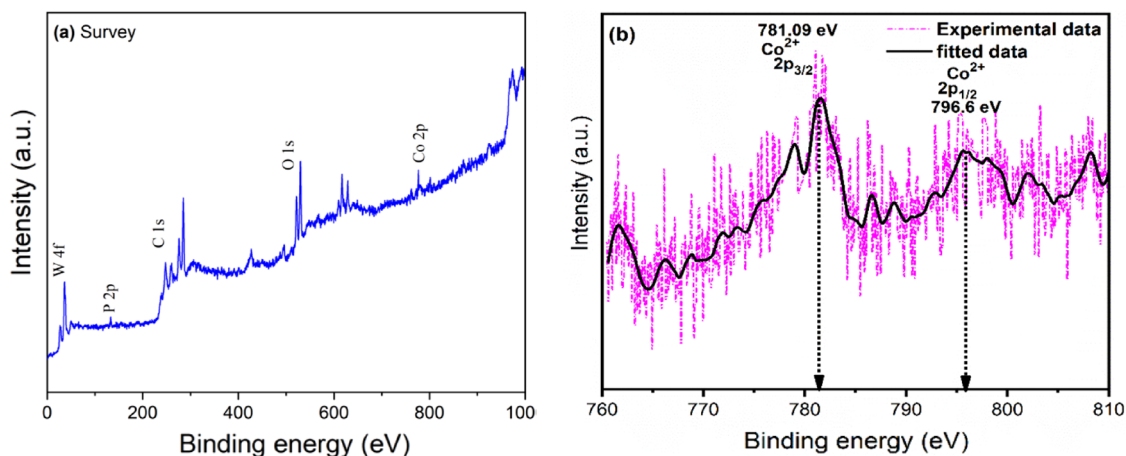


Fig. 8 XPS of PDPA-PWCo hybrid material, (a) survey spectrum showing elements present in the hybrid and (b) Co^{2+} 2p spectrum

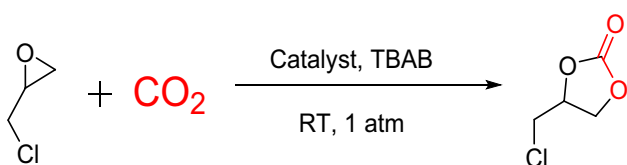
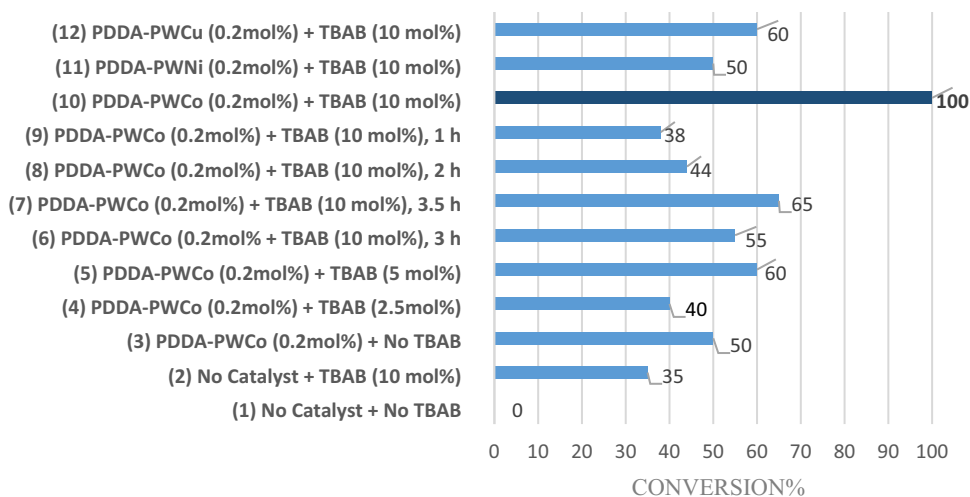
moiety. The presence of Co^{2+} in an octahedral site of Keggin is further evidenced from the XP spectrum, as Fig. 8b shows the peaks at 781.09 and 796.6 eV corresponding to Co^{2+} 2p_{3/2} and Co^{2+} 2p_{1/2}, respectively.

3.2 Conversion of CO_2 to Cyclic Carbonates Using PDPA-TMSPOM Catalysts

The hybrid materials, PDPA-TMSPOMs, are used as heterogeneous catalysts for the conversion of carbon dioxide to cyclic carbonates under mild reaction conditions. The reaction has been carried out by mixing epoxide (5 mmol), TBAB as co-catalyst (0.5 mmol) and PDPA-TMSPOM catalyst (0.2 mol%) in a round bottom flask that is fitted

with a rubber stopper pierced by a balloon that contains CO_2 . This cycloaddition reaction is allowed to run for 4 h at room temperature. At the completion of the reaction, the work up is done by adding ethyl acetate to the reaction mixture. The catalyst is recovered by centrifugation and the organic part is collected. The collected organic part is washed with water and dried over anhydrous Na_2SO_4 . The desired product is obtained by evaporating the ethyl acetate solvent. The final cyclic carbonate product is analyzed by NMR analysis to determine the conversion. The substrate conversion and the selectivity are based on ^1H -NMR of crude reaction mixture during the optimization, substrate scope and recyclability studies. The results are summarized in Chart 1. All the reactions are carried out

Chart 1 Cycloaddition of CO₂ to epoxides. Optimization studies reveal that the combination of PDDA-PWCo (0.2 mol%) and TBAB (10 mol%) is the best catalytic system for 100% conversion under ambient reaction conditions. All reactions are carried out for 4 h (except for entry 6–9)



Scheme. 1 Cycloaddition of CO₂ to epichlorohydrin to give corresponding cyclic carbonate

under solvent-free conditions for 4 h (except for entry 7 (3.5 h) and 8 (3 h) in Chart 1).

Initially, we tested the cycloaddition of CO₂ to epichlorohydrin (Scheme 1). The reaction with no catalyst and co-catalyst does not give the desired product (Chart 1: entry 1). In the absence of PDDA-PWCo, TBAB gave only 35% conversion of the epoxide to the corresponding cyclic carbonate are observed whereas PDDA-PWCo gave 50% conversion in the absence of TBAB (Chart 1: entry 2 and 3). This clearly indicates that the hybrid catalysts are more efficient to carry out this cycloaddition. Interestingly, in the presence of the catalytic system comprising of PDDA-PWCo (0.2 mol%) and TBAB (0.5 mmol), the reaction resulted in 100% conversion of epichlorohydrin, producing desired cyclic carbonate (Chart 1: entry 10). The result indicates that the reaction proceeds smoothly with high selectivity without the formation of side-products. Comparatively, the combinations of PDDA-PWCo/TBAB and PDDA-PWCo/TBAB gave 60% and 50% of conversion, respectively (Chart 1: entry 11 and 12; comparative ¹H NMR spectra in Figure S1). As the reaction progressed over the course of 1 and 2 h, respectively, 38% and 44% conversion was observed. Furthermore, the conversion was 55% after 3 h and 65% after 3.5 h. (comparative ¹H NMR spectra in Figure S2). When the co-catalyst loading is decreased to 0.125 mmol and 0.25 mmol, the epichlorohydrin conversion is found to decrease to 60% and

40%, respectively (Chart 1: entry 4 and 5; comparative NMR spectra in Figure S3).

The screening studies show that the PDDA-PWCo in combination with TBAB has emerged as the best choice to give higher conversion of epoxide with high selectivity (Chart 1). The higher catalytic activity of PDDA-PWCo is attributed to the higher affinity of cobalt towards binding with epoxides [36]. The confined space of the layered PDDA-PWCo interlayer region may induce some restrictions in the overall structure and this may have resulted in controlling the accessibility of the catalytic active site in the interlayer region, leading to the increased catalytic activity of PDDA-PWCo. The catalytic ability of substituted Co²⁺ POM is shown in some reports [37, 38]. To further confirm the catalytic potential of PDDA-PWCo, recyclability studies have been carried out which revealed that this binary catalytic system gives better results even after fourth reuse under mild reaction conditions (Chart 2, for comparison ¹H-NMR in Figure S4).

The reaction conditions employed herein are economically viable and most convenient to carry out. Hence these conditions are applied to reactions involving structurally diverse epoxides by using 0.2 mol% of PDDA-PWCo catalyst without any solvent at room temperature. The results are summarized in Table 1. The cycloaddition of CO₂ to propylene oxide, epoxyhexane, cyclopentene oxide, epoxy-cyclohexane and styrene oxide proceeds efficiently giving better conversion of epoxides to the corresponding cyclic carbonates under eco-friendly reaction conditions than similar reactions reported in the literature. Interestingly, octadiene diepoxide produced efficiently corresponding cyclic dicarbonate, a result that bodes well for future uses of such fascinating compounds.

We have compared the catalytic activity of PDDA-PWCo catalyst with some of the previously disclosed POM-based catalysts used for synthesizing cyclic carbonates at room

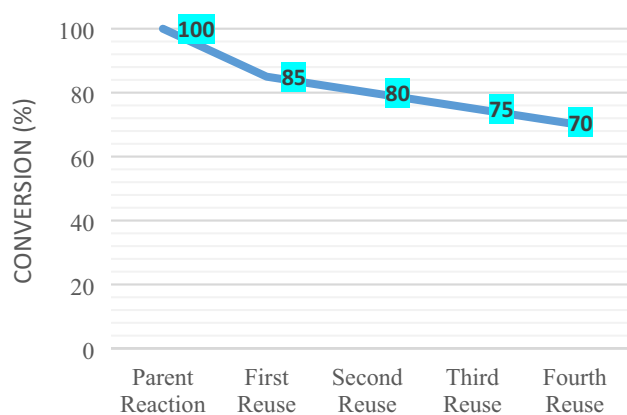
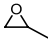
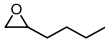
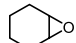
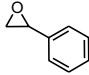
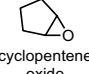
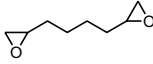


Chart 2 Recyclability studies of PDDA-PWCo/TBAB catalyst for cycloaddition of CO₂ to epoxides. Reaction conditions: PDDA-PWCo (0.2 mol%), TBAB (10 mol%), epoxide (1 mmol), CO₂ (1 atm.), RT, 4 h

Table 1 Cycloaddition reaction of CO₂ with different epoxides using PDDA-TMSPOM under solvent-free conditions at room temperature

S. No.	Substrate	Reaction time (h)	Conversion [#] (%)
1.	 propylene oxide	4	78
2.	 Epoxyhexane	4	65
3.	 Epoxy cyclohexane	4	57
4.	 Styrene oxide	4	50
5.	 cyclopentene oxide	4	60
6.	 1, 7-octadiene diepoxide	4	60

[#]based on ¹H-NMR analysis

Reaction conditions: PDDA-PWCo (0.2 mol%) and TBAB (10 mol%), Epoxide (1 mmol), CO₂ (1 atm.), RT, 4 h

temperature with no solvent [39–43]. This comparative data is summarized in Table 2 for the reaction of epichlorohydrin and CO₂. The reactions referred in Table 2 require higher temperatures and CO₂ pressure. The PDDA-PWCo catalyst demonstrates comparatively better catalytic efficiency towards cyclic carbonates, as can be seen in Table 2. The reason for better activity of cobalt substituted hybrid seems to be the affinity of cobalt towards binding with epoxides

[36]. Moreover, the surface area of PDDA-PWCo is 13 m²/g whereas PDDA-PW_{Ni} and PDDA-PW_{Cu} catalysts have surface areas of 5 m²/g and 8 m²/g, respectively. Thus, comparatively higher surface area could be another reason for better activity of PDDA-PWCo than its competitive hybrid catalysts reported here.

The plausible mechanism is shown in Scheme 2 that involves the epoxide activation by Lewis acidic hybrid material such as PDDA-PWCo. The catalyst activates the oxirane ring through the interaction with the oxygen atom to facilitate the nucleophilic attack of TBAB on the epoxide ring. The attack of bromide leads to the ring opening and at this stage, CO₂ insertion in the metal alkoxide bond occurs. Finally, the intra-molecular cyclization accompanied with the removal of bromide leads to the generation of the cyclic carbonate [44, 45].

The catalytic approach developed in this study does not require any solvent and the products can be obtained in a short duration at room temperature. This clearly demonstrates that the transition metal substituted monolacunar catalytic systems are useful to synthesize cyclic carbonates under environmentally benign conditions. Finally, this catalytic process can be useful for industrial targets involving bio-based cyclic carbonate products.

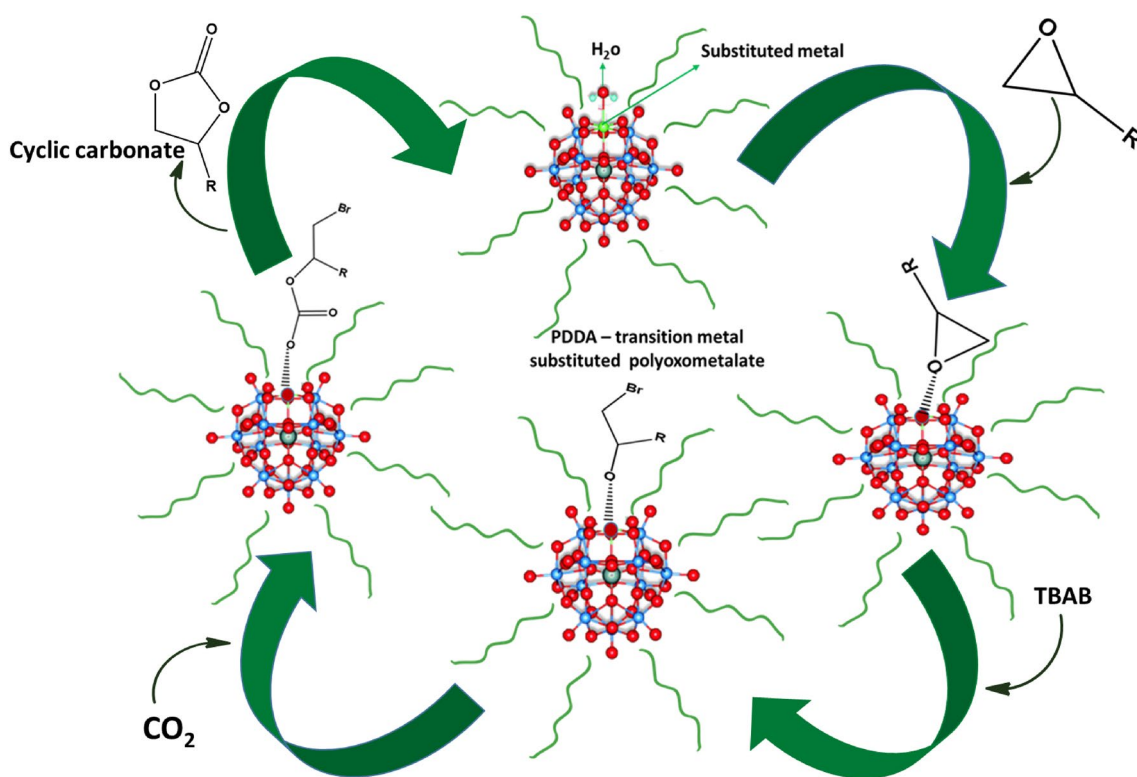
4 Conclusions

In summary, we have synthesized three hybrid catalytic materials consisting of Cu²⁺, Co²⁺, and Ni²⁺ ion substituted Keggin structures and PDDA polymer matrix (PDDA-TMSPOMs). The formation of transition metal substituted Keggin anions are evident from FTIR and UV–Visible spectra, and further confirmed by TGA and ³¹P NMR. The TGA analysis also showed the extended thermal stability of the materials upto 400 °C. The powder XRD pattern revealed the amorphous nature of all the three hybrid materials while the irregular surface morphology can be seen in SEM images. Among the POM-based hybrid catalytic materials, PDDA-PW_{Cu}, PDDA-PW_{Ni} and PDDA-PW_{Co}, PDDA-PW_{Co} is the most efficient heterogeneous catalyst for synthesizing cyclic carbonates under eco-friendly reaction conditions. This catalytic approach provides the cyclic carbonates in good yields under solvent-free conditions with 100% selectivity. Furthermore, the reported synthetic approach here requires no column purification of products, and thus, avoids tedious methods and waste generation. Considering these factors, PDDA-PW_{Co}-catalyzed synthesis of cyclic carbonates truly stands as an environmentally friendly catalytic method towards potentially useful chemicals.

Supplementary Information The online version contains supplementary material available at <https://doi.org/10.1007/s10562-023-04392-1>.

Table 2 Comparison of catalytic activities of CO₂ conversion to cyclic carbonates

Catalyst/Co-catalyst	Temp. (°C)	CO ₂ Pressure (atm.)	Reaction time (h)	Conversion (%)	Ref
Zn-POMOF (2 mol%)/TBAB (2.5 mol%)	80	10	12	92	[41]
[Na(H ₂ O) ₅](NH ₄) ₇ [P ₂ W ₁₅ O ₅₆ Co ₃ –(H ₂ O) ₃ (OH) ₃ Mn(CO) ₃]·19H ₂ O (0.23 mol%)/pyrrolidinium bromide (8 mol%)	70	15	1.5	96	[42]
Na _{1.5} H _{4.5} [(CH ₃) ₄ N] ₂ [Mn(CO) ₃] ₄ (Se ₂ W ₁₁ O ₄₃)·9H ₂ O (0.15 mol%)/1-ethyl-1-methylpyrrolidinium bromide (8 mol%)	70	15	1	94.7	[43]
Cr-MIL-101 (50 mg) TBAB (0.31 mmol)	25	8	24	91	[39]
Ce ₂ NDC ₃ (15 mg) TBAB (1.8 mol %)	25	1	8	92	[40]
PDDA-PWCo (0.2 mol%)/TBAB (0.5 mmol)	25	1	4	100	This Work

**Scheme 2** Mechanism of cycloaddition of CO₂ to epoxides to form cyclic carbonates using PDDA-TMSPOM catalytic clusters

Acknowledgements RJ would like to express gratitude to Prof. Ranga Rao for providing research facilities to carry out this work in DSEHC-Solar Fuels Laboratory at IIT Madras. DSEHC is supported by Department of Science and Technology, Government of India through Grant No. DST/TMD/SERI/HUB/1(C). RJ, CAB, RRS and KS acknowledge BSACIST for research facilities for a part of this work.

Author Contributions RJ, CAB: material preparation, data collection, early draft and analysis; RRS: study conception; KS: materials design; RRS and KS: study design, monitoring, data analysis, manuscript draft

preparation, editing; GRR: Funding, study design, monitoring and final editing.

Declarations

Conflict of interest The authors have no relevant conflicts of interests to disclose.

References

1. Truong CC, Mishra DK (2020) *Environ Chem Lett* 19:911–940. <https://doi.org/10.1007/s10311-020-01121-7>
2. Osman AI, Hefny M, Abdel Maksoud MIA, Elgarahy AM, Rooney DW (2020) *Environ Chem Lett* 19:797–849. <https://doi.org/10.1007/s10311-020-01133-3>
3. Peng J, Geng Y, Yang HJ, He W, Wei Z, Yang J, Guo C-Y (2017) *Mol Catal* 432:37–46. <https://doi.org/10.1016/j.mcat.2017.01.019>
4. Chen X, Liu Y, Wu J (2020) *Mol Catal* 483:110716. <https://doi.org/10.1016/j.mcat.2019.110716>
5. Corma A, Garcia H (2013) *J Catal* 308:168–175. <https://doi.org/10.1016/j.jcat.2013.06.008>
6. Zhang YY, Yang GW, Xie R, Yang L, Li B, Wu GP (2020) *Angew Chem Int Ed* 59:23291–23298. <https://doi.org/10.1002/anie.202010651>
7. Lang X-D, He LN (2016) *Chem Rec* 16:1337–1352. <https://doi.org/10.1002/tcr.201500293>
8. Zhai G, Liu Y, Lei L, Wang J, Wang Z, Zheng Z, Wang P, Cheng H, Dai Y, Huang B (2021) *ACS Catal* 11:1988–1994. <https://doi.org/10.1021/acscatal.0c05145>
9. Miao CX, Wang JQ, Wu Y, Du Y, He LN (2008) *Chemoschem* 1:236–241. <https://doi.org/10.1002/cssc.200700133>
10. Cao JP, Xue YS, Li NF, Gong JJ, Kang RK, Xu Y (2006). *J Am Chem Soc.* <https://doi.org/10.1021/9781420015751>
11. Mizuno N, Kamata K, Yamaguchi K (2006) *Surface and Nanomolecular Catalysis*. In: Richards Ryan (ed) *Liquid-phase oxidations catalysed by polyoxometalates*. CRC Press Taylor and Francis, Boca Raton, pp 463–492
12. Chen F, Li X, Wang B, Xu T, Chen SL, Liu P, Hu C (2012) *Chem Eur J* 18:9870–9876. <https://doi.org/10.1002/chem.201201042>
13. Wang Y, Wu Z, Yu H, Han S, Wei Y (2020) *Green Chem* 22:3150–3154. <https://doi.org/10.1039/d0gc00388c>
14. Yu B, Zou B, Hu CW (2018) *J CO2Util* 26:314–322. <https://doi.org/10.1016/j.jcou.2018.05.021>
15. Wang SS, Yang GY (2015) *Chem Rev* 115:4893–4962. <https://doi.org/10.1021/cr500390v>
16. Miras HN, Yan J, Long DL, Cronin L (2012) *Chem Soc Rev* 41:7403. <https://doi.org/10.1039/c2cs35190k>
17. Pattnaik F, Tripathi S, Patra BR, Nanda S, Kumar V, Dalai AK, Naik S (2021) *Environ Chem Lett* 19:4119–4136. <https://doi.org/10.1007/s10311-021-01284-x>
18. Long DL, Tsunashima R, Cronin L (2010) *Angew Chem Int Ed* 49:1736–1758. <https://doi.org/10.1002/anie.200902483>
19. Nsouli NH, Ismail AH, Helgadottir IS, Dickman MH, Clemente-Juan JM, Kortz U (2009) *Inorg Chem* 48:5884–5890. <https://doi.org/10.1021/ic900180x>
20. Xiao Y, Chen D, Ma N, Hou Z, Hu M, Wang C, Wang W (2013) *RSC Adv* 3:21544. <https://doi.org/10.1039/c3ra43373k>
21. Qi W, Wu L (2009) *Polym Int* 58:1217–1225. <https://doi.org/10.1002/pi.2654>
22. Chen H, Wang Y, Dong S (2007) *Inorg Chem* 46:10587–10593. <https://doi.org/10.1021/ic7009572>
23. Ge W, Wang X, Zhang L, Du L, Zhou Y, Wang J (2016) *Catal Sci Technol* 6:460–467. <https://doi.org/10.1039/c5cy01038a>
24. Zhao YQ, Liu YY, Ma JF (2020) *Cryst Growth Des* 21:1019–1027. <https://doi.org/10.1021/acs.cgd.0c01353>
25. Shakeela K, Sinduri VL, Ranga Rao G (2017) *Polyhedron* 137:43–51. <https://doi.org/10.1016/j.poly.2017.07.023>
26. Shakeela K, Ranga Rao G (2018) *ACS Appl Nano Mater* 1:4642–4651. <https://doi.org/10.1021/acsnm.8b00920>
27. Houston JE, Patterson AR, Jayasundera AC, Schmitt W, Evans RC (2014) *Chem Commun* 50:5233–5235. <https://doi.org/10.1039/c3cc47552b>
28. Zhao W, Yang C, Cheng Z, Zhang Z (2016) *Green Chem* 18:995–998. <https://doi.org/10.1039/c5gc02527c>
29. Shakeela K, Guru S, Ranga Rao G (2020). *J Chem Sci.* <https://doi.org/10.1007/s12039-020-01804-2>
30. Han F, Li H, Zhuang H, Hou Q, Yang Q, Zhang B, Miao C (2021) *J CO2 Util* 53:101742. <https://doi.org/10.1016/j.jcou.2021.101742>
31. Simões MMQ, Conceição CMM, Gamelas JAF, Domingues PMDN, Cavaleiro AMV, Cavaleiro JAS, Ferrer-Correia AJV, Johnstone RAW (1999) *J Mol Catal A Chem* 144:461–468. [https://doi.org/10.1016/s1381-1169\(99\)00025-4](https://doi.org/10.1016/s1381-1169(99)00025-4)
32. Zhang Q, An Q, Luan X, Huang H, Li X, Meng Z, Tong W, Chen X, Chu PK, Zhang Y (2015) *Nanoscale* 7:14002–14009. <https://doi.org/10.1039/c5nr03256c>
33. Rajkumar T, Ranga Rao G (2009) *J Chem Sci* 120:587–594. <https://doi.org/10.1007/s12039-008-0089-x>
34. Levine DJ, Stöhr J, Falese LE, Ollesch J, Wille H, Prusiner SB, Long JR (2015) *ACS Chem Biol* 10:1269–1277. <https://doi.org/10.1021/cb5006239>
35. Patel K, Shringarpure P, Patel A (2010) *Transit Met Chem* 36:171–177. <https://doi.org/10.1007/s11243-010-9450-2>
36. Lu X-B, Wang Y (2004) *Angew Chem Int Ed* 43:3574–3577. <https://doi.org/10.1002/anie.200453998>
37. Singh C, Mukhopadhyay S, Das S (2018) *Inorg Chem* 57:6479–6490. <https://doi.org/10.1021/acs.inorgchem.8b00541>
38. Mulkapuri S, Ravi A, Das S (2022) *Chem Mater* 34:3624–3636. <https://doi.org/10.1021/acs.chemmater.1c03917>
39. Zalomaeva OV, Chibiryaev AM, Kovalenko KA, Kholdeeva OA, Balzhinimaev BS, Fedin VP (2013) *J Catal* 298:179–185. <https://doi.org/10.1016/j.jcat.2012.11.029>
40. Das SK, Chatterjee S, Bhunia S, Mondal A, Mitra P, Kumari V, Pradhan A, Bhaumik A (2017) *Dalton Trans* 46:13783–13792. <https://doi.org/10.1039/c7dt02040f>
41. Cheng W, Xue Y, Luo X-M, Xu Y (2018) *Chem Commun* 54:12808–12811. <https://doi.org/10.1039/c8cc07041e>
42. Jia J, Niu Y, Zhang P, Zhang D, Ma P, Zhang C, Niu J, Wang J (2017) *Inorg Chem* 56:10131–10134. <https://doi.org/10.1021/acs.inorgchem.7b01231>
43. Lu J, Ma X, Singh V, Zhang Y, Wang P, Feng J, Ma P, Niu J, Wang J (2018) *Inorg Chem* 57:14632–14643. <https://doi.org/10.1021/acs.inorgchem.8b02321>
44. Szczepankiewicz SH, Ippolito CM, Santora BP, Van de Ven TJ, Ippolito GA, Fronckowiak L, Wiatrowski F, Power T, Kozik M (1998) *Inorg Chem* 37:4344–4352. <https://doi.org/10.1021/ic980162k>
45. Khenkin AM, Efremenko I, Weiner L, Martin JML, Neumann R (2010) *Chem Eur J* 16:1356–1364. <https://doi.org/10.1002/chem.200901673>

Publisher's Note Springer Nature remains neutral with regard to jurisdictional claims in published maps and institutional affiliations.

Springer Nature or its licensor (e.g. a society or other partner) holds exclusive rights to this article under a publishing agreement with the author(s) or other rightsholder(s); author self-archiving of the accepted manuscript version of this article is solely governed by the terms of such publishing agreement and applicable law.

Authors and Affiliations

Rehana Jan¹ · Christy Ann Biji² · K. Shakeela¹  · Rafik Rajjak Shaikh¹  · G. Ranga Rao³

✉ K. Shakeela
shakeelakhann@gmail.com

✉ Rafik Rajjak Shaikh
rafik.shaikh@crecident.education

¹ Department of Chemistry, B.S. Abdur Rahman
Crescent Institute of Science and Technology,
Vandalur, Chennai 600048, India

² Department of Chemistry, Madras Christian College, East
Tambaram, Chennai 600059, India

³ Department of Chemistry and DST-Solar Energy Harnessing
Centre (DSEHC), Indian Institute of Technology Madras,
Chennai 600036, India